Pressure Drop Analysis of Direct Liquid Cooled (DLC) Rack

Sami Alkharabsheh*, Bharath Ramakrishnan, Bahgat Sammakia
State University of New York at Binghamton
Binghamton, NY, USA, 13850
*Email: salkhar1@binghamton.edu

ABSTRACT

This study presents an experimental and numerical characterization of pressure drop in a commercially available direct liquid cooled (DLC) rack. It is important to investigate the pressure drop in the DLC system as it determines the required pumping power for the DLC system, which affects the energy efficiency of the data center. The main objective of this research is to assess the flow rate and pressure distributions in a DLC system to enhance the reliability and the cooling system efficiency. Other objectives of this research are to evaluate the accuracy of flow network modeling (FNM) in predicting the flow distribution in a DLC rack and identify manufacturing limitations in a commercial system that could impact the cooling system reliability.

The main components of the investigated DLC system are: coolant distribution module (CDM), supply/return manifold module, and server module which contains a cold plate. Extensive experimental measurements were performed to study the flow distribution and to determine the pressure characteristic curves for the server modules and the coolant distribution module (CDM). Also, a methodology was described to develop an experimentally validated flow network model (FNM) of the DLC system to obtain high accuracy.

The measurements revealed a flow maldistribution among the server modules, which is attributed to the manufacturing process of the micro-channel cold plate. The average errors in predicting the flow rate of the server module and the CDM using FNM are 2.5% and 3.8%, respectively. The accuracy and the short run time make FNM a good tool for design, analysis, and optimization for DLC systems. The pressure drop in the server module is found to account for 56% of the total pressure drop in the DLC rack. Further analysis showed that 69% of the pressure drop in the server module is associated with the module's plumbing (corrugated hoses, disconnects, fittings). The server cooling modules are designed to provide secured connections and flexibility, which come with a high pressure drop cost.

KEYWORDS

Data center, liquid cooling, warm water cooling, cold plate, pressure drop, flow network modeling (FNM)

NOMENCLATURE

CDM	coolant distribution module
CFD	computational fluid dynamics
D	hydraulic diameter (m)
DAQ	data acquisition
DLC	direct liquid cooling
FNM	flow network modeling
K	loss coefficient
KVL	Kirchhoff's voltage law
L	pipe length (m)
p	pressure (Pa)
PID	proportional–integral–derivative
PUE	power usage effectiveness
PGW	propylene glycol water
ρ	fluid density (kg/m^3)
RU	rack unit
Q	flow rate (m^3/s)
v	velocity (m/s)
v_{cb}	potential difference (V)

INTRODUCTION

There has been a tremendous focus on data center energy efficiency after about a decade of the "Report to Congress on Server and Data Center Energy Efficiency" prepared by the United States Environmental Protection Agency (EPA) in 2007 [1]. This focus resulted in stabilizing the power consumption in data centers, in spite of the continuous growth in the data center industry. A recent survey [2] showed that the data center electricity use in 2014 is only 4% more than that in 2010 and stayed at 1.8% of total electricity use. This is a big improvement compared with the change in electricity use in 2005-2010 (24%) and 2000-2005 (90%), as shown in Figure 1. The same survey also indicated that the percentage increase in electricity use will maintain at 4% toward 2020 while the total server installed base is projected to increase by 40% from 2010 to 2020. Furthermore, the current trend can be reduced by 45% through

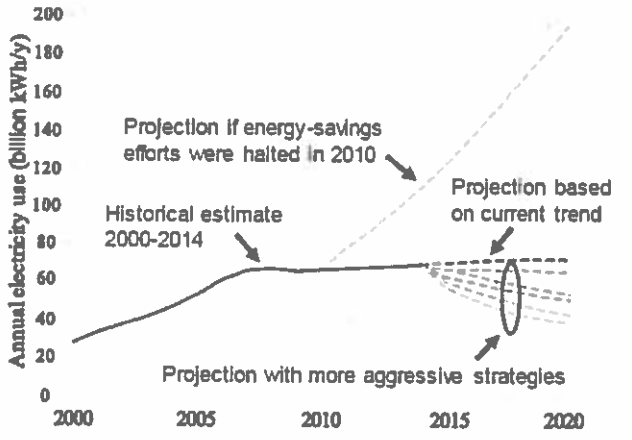

Figure 1: Current and projected data center total electricity use [2]

adopting different aggressive energy efficiency strategies (improved management, best practices, hyperscale shift).

Cooling was reported to consume 30%-40% of the total energy used in legacy data centers [3]. Despite the optimistic results for the current trends [2], the average power usage effectiveness (PUE) is reported to be 1.8 in 2013 [4] mostly due to inefficiencies in the cooling system. Several thermal management technologies are used in data centers cooling to address the inefficiency challenges [5]. The most widely used cooling systems are: cold/hot aisle containment [6], air-side economization [7], rack level hybrid cooling [8] and liquid cooling [9].

The notion of cooling electronic systems using liquids is not novel, however, potential leaks and the capital cost have greatly restricted its application in real data centers [10-12]. In direct liquid cooling (DLC) technology a liquid cooled cold plate is situated on top of a chip, which reduces the thermal resistance between the chip junction and the cooling source, and provides an opportunity to enhance the thermal efficiency of the cooling system. A study showed that for computationally equivalent clusters, DLC can save 45% energy compared with standard hot/cold aisle air cooling [13]. The low thermal resistance path encouraged designs to operate at higher coolant temperatures (known as warm-water cooling) in which a water side economizer utilizing ambient temperature replaces a chilled water system gaining savings more than 90% [14-15]. Despite of the perception of using liquid in cooling data centers, the potential 'big energy savings using DLC encouraged the industry to develop commercial products that can be used in data centers [16-17].

There are many research studies in literature focused on the pressure drop in liquid cooled cold plates. These studies are outside the scope of this study as this research focuses on the system level problem (particularly rack level). Few studies in literature have focused on the system level analysis of DLC, these studies mainly investigated the thermal performance such as the effect of coolant inlet temperature, flow rate, ambient temperature and chip power on the cooling of the DLC system [18-20]. Pressure drop analysis of DLC systems is important to study, as it determines the required pumping power for the DLC system, which affects the energy consumption of the cooling system and the energy efficiency of the data center.

Flow network modeling is an effective tool to study the flow and pressure drops in complex flow networks [21, 22]. The accuracy of this method depends on using accurate pressure drop characteristic of each element in a system, which can be obtained experimentally or using computational fluid dynamics (CFD). In a relevant study [23], flow network software Macroflow™ [24] is used for flow analysis at the design stage of a direct liquid cooled rack and obtained agreement with measurements within 5%.

This research addresses the research gap in characterizing the pressure drop in a direct liquid cooled rack. Experimental measurements and numerical modeling using flow network model are used in this analysis. The major outcome from this work is to identify the components with high pressure drops therefore they can be targeted in optimization studies to reduce the pressure drop and consequently the pumping power to enhance the cooling system efficiency. Other outcomes are to demonstrate some limitations in the manufacturing process that could lead to a risky flow maldistribution. Additionally, this study defines a methodology to model a liquid cooled rack using a flow network model and determines the resulting accuracy. Furthermore, the resulting flow analysis is required for future thermal analysis of this system.

SYSTEM DESCRIPTION

The tested system is a commercially available rack level direct liquid cooling (DLC) solution for data centers [25]. This system consists of two main loops: the primary loop and the secondary loop, as shown in Figure 2. The purpose of the primary loop is to carry the heat from the rack and to dispose of it in the environment outside the data center. It consists mainly of a flow regulating valve with a proportional–integral–derivative controller (PID controller), facility side piping system and a dry cooler (for chillerless systems) or a chiller (for chilled water systems). The primary loop in this study is connected to a chilled water system for future research purposes. For instance, by changing the chilled water supply temperature, the ambient temperature can be simulated experimentally to study the thermal performance of this system under different environmental conditions.

The purpose of the secondary loop is to carry the heat from the chips inside the servers (via direct contact cold plates) and to dispose of it in the primary loop. The coolant in the secondary loop is propylene glycol (15%) water (85%) mixture. The secondary loop consists of three modules: (a) coolant distribution module (CDM) (b) supply and return manifolds module (c) server module. The CDM in Figure 3a contains a liquid to liquid heat exchanger, two recirculation pumps in series (for redundancy), coolant reservoir, flow meter, and temperature and pressure sensors at the supply and return lines.

The manifold module in Figure 3b is six feet long with square cross section and is made of a stainless material. The manifold can accommodate 42 server modules connected in parallel using dry-break quick disconnect sockets. The server module in Figure 3c consists of corrugated hoses, fittings, dry-break quick disconnect plugs and the microchannel cold plate component. It is important in this study to understand that the server module not only contains the cold plate but also it has the attached plumbing. The cold plate component consists of a plastic cover and a copper microchannel heat sink, as shown in Figure 3d. The copper heat sink contains a V-groove to split the impinging jet between two sets of parallel channel. This

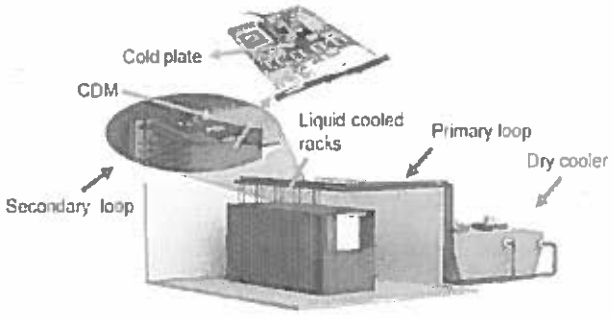

Figure 2: Direct liquid cooling system under investigation [26]

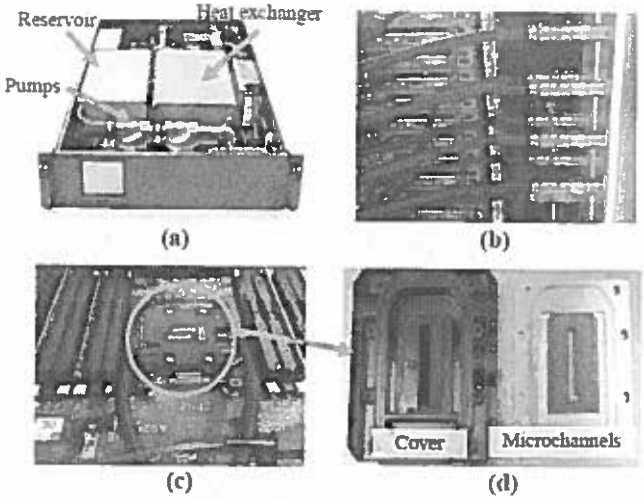

Figure 3: The three modules of the secondary loop: (a) coolant distribution module (courtesy of CoolIT Systems) (b) manifold module (c) server module (d) microchannel cold plate component

manufacturer's design ensures low pressure drop and thermal resistance. There are other related studies focused on experimental and numerical analysis of this microchannel cold plate [27, 28].

EXPERIMENTAL SETUP

The experimental setup is located inside the Binghamton University data center laboratory. The data center contains 41 racks divided between three cold aisles with a total area of 215 m2. A rack level DLC is installed on one of the racks to perform this experiment. Since this experiment is located inside a data center, it requires a careful planning to securely install the sensors without causing liquid leak. The sensors were installed in manifolds equipped with dry-break quick disconnects of the same type which is used by the manufacturer of the DLC, as shown in Figure 4(a,b). By doing that, the sensors can be integrated with the rack tubing without introducing possible leak locations in the system. Furthermore, the measuring manifolds were introduced to a pressure test to ensure the design integrity under different conditions.

The instruments used in this experiments are:

- Micro-flow meter: OMEGA FTB-314D, flow rate range 0.3-3.0 l/min and accuracy ±6% full scale.
- Pressure gauges: OMEGA MMG100V10P3A0T3A5, range: 0-100psi, accuracy ±0.08% (used for high pressure measurements)
- Differential pressure transducer: OMEGA PX2300-5DI, range: 0-5psi, accuracy ±0.25% (used for low pressure measurements)
- Thermocouples: OMEGA J-type thermocouple probe
- Data acquisition (DAQ): Agilent 34980A

The micro-flow meter is recalibrated in-house as the factory calibration is based on water, while the fluid in our case is propylene glycol water mixture. Graduated cylinder-stop watch standard testing is used for this purpose. The thermocouples are

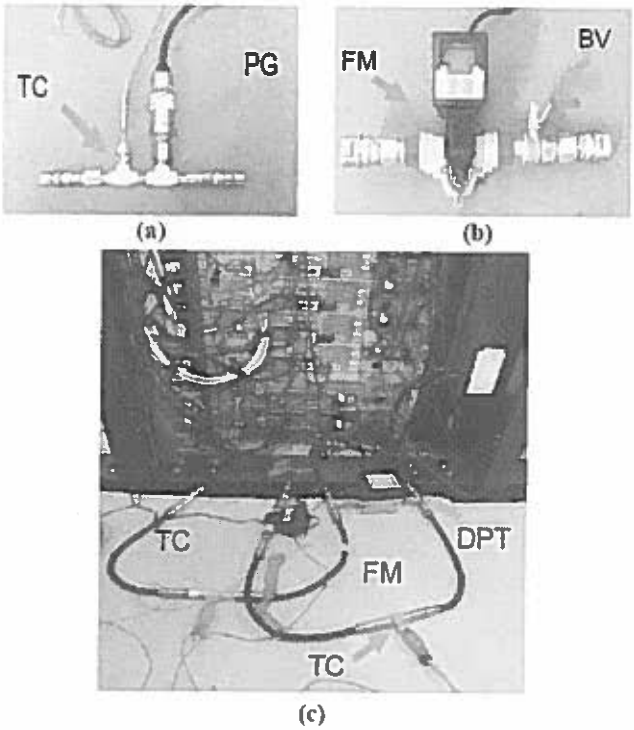

Figure 4: Measurement sensors: (a) Pressure gage (PG) and thermocouple (TC) (b) Micro-flow meter (FM) and ball valve (BV) (c) Sample experiment inside the data center (DPT: differential pressure transducer)

included in this study, since it is expected that with temperature variations the pressure drop will change due to viscosity change. Figure 4c shows the experimental setup inside the data center for testing one of the servers.

The rack is equipped with 14 2RU servers, the used notation for servers in later sections is 1 to 14 from top to bottom of the rack (server 1: top of the rack, server 14: bottom of the rack). Servers 2-13 are Dell R520 and servers 1&14 are Dell R730. While both kind of servers contain two CPUs, the internal architecture is different. Therefore, to accommodate the liquid cooling module inside the server, the tubing, and the fittings must be customized based on the available space inside each server. Server 1 is equipped with a dual head server module indicating that two cold plates are connected in series and share the same cooling source (denoted by Type A), as shown in Figure 5a. Servers 2-13 are also equipped with a dual head server module shown in Figure 5b (denoted by Type B). The differences between the dual head modules in server 1 and servers (2-13) is in the angle of the fittings and the length of the hoses to fit inside the server. Server 14 is equipped with two single head server modules shown in Figure 5c indicating that each CPU in the server gets the cooling independently from the rack manifold (denoted by Type C). The server modules for server 14 are denoted by 14-1 and 14-2.

The data collection in this study is based on taking real time measurements from all sensors then using the average value as a data point. For consistency, 120 samples are collected over 10 minutes (5 seconds time step) for all the data points in this experiment.

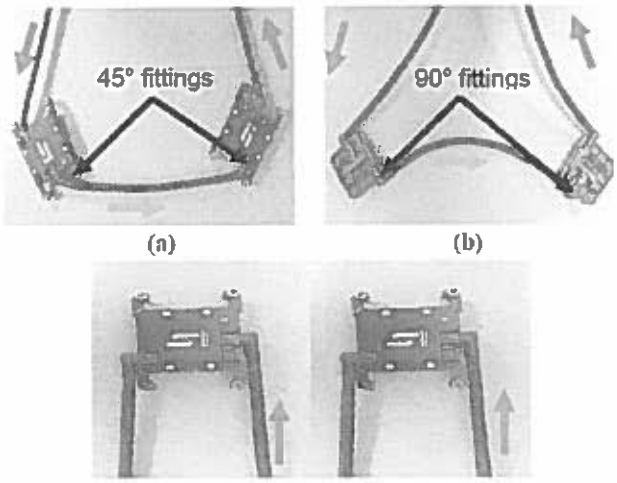

Figure 5: Different server modules used in the DLC racks (a) Type A: dual head 45°C (b) Type B: dual head 90°C (c) Type C: single head

FLOW ANALYSIS

This section presents experimental measurements to understand the flow rate distribution in the DLC rack and the corresponding pressure drop in the server modules.

The flow rate distribution in the server modules is shown in Figure 6. Based upon the description of the installed server modules in the Experimental Setup section, the pressure drop in Type B is expected to be the highest followed by Type A and then Type C. The reason is Type A has two cold plates with 45° fittings angle, Type B has two cold plates with 90° fittings angle and Type C has a single cold plate. This agrees with the general flow distribution in Figure 6. However, the surprising behavior is in the noticeable flow maldistribution between Type B server modules (2-13). The ratio of the lowest flow rate (module 2) to the highest flow rate (module 9) is as big as 63%.

To understand what causes the flow maldistribution, the impedance curve for each of the 15 modules in the rack is measured. The results in Figure 7 suggest that the there is a variation in the pressure characteristics in the server modules (2-13) although they all are of Type B. The results for (14-1 & 14-2) are as it would be expected.

The variation in the pressure drop of server modules (2-13)

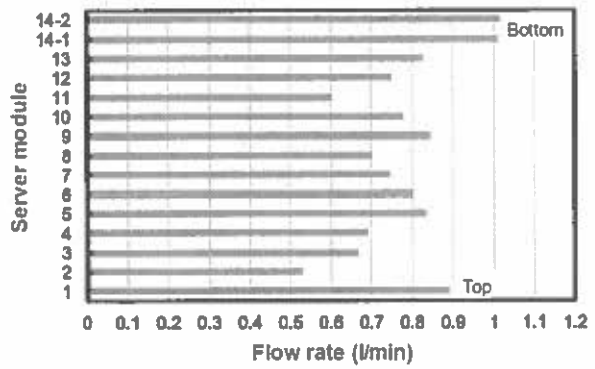

Figure 6: Flow rate distribution in the server modules (1: top server module, 14-2: bottom server module)

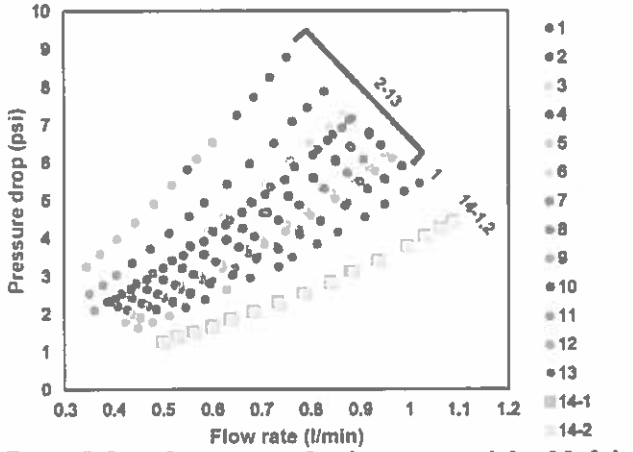

Figure 7: Impedance curves for the server modules. Module 1-13 are dual head and 14-1, 2 are single head

can be attributed to the micro-channel cold plate or the attached plumbing (disconnects and hoses). It is unfeasible to conduct destructive testing for 13 modules to specify which part of the server module responsible for this variation. Instead, we inspected the pressure drop in the plumbing part using jumper hoses that include the same type of hoses and disconnects as that in the server module, as shown in Figure 8a. Six jumper hoses were tested and found that they have consistent pressure characteristics, as shown in Figure 8b. This finding excludes the plumbing part leaving the cold plate component as the only component that can cause the variation in pressure drop in

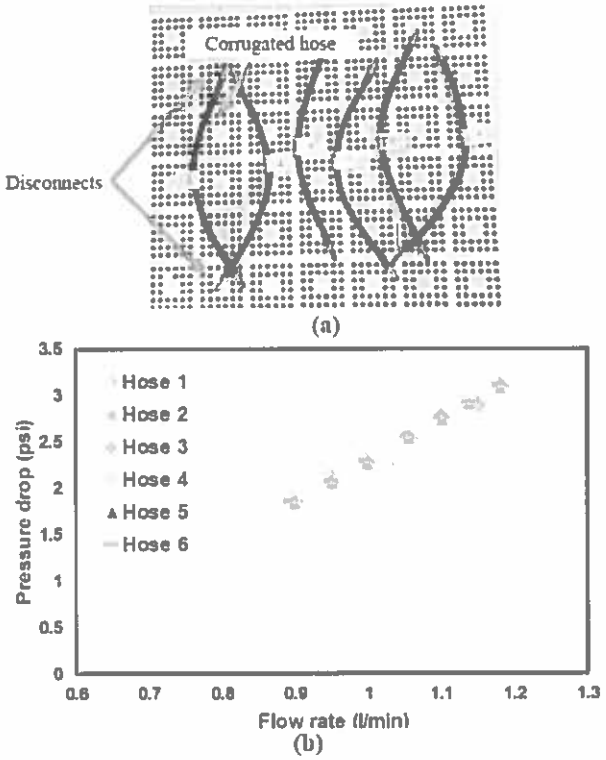

Figure 8: (a) Jumper hoses with same tubing and disconnects as the server module (b) Pressure drop characteristics

Figure 7. This variation is attributed to the manufacturing process of the micro-channel cold plate. The flow maldistribution is risky on the reliability of the IT equipment and makes the optimization of cooling system challenging. This can be addressed by precise manufacturing and exposing the microchannel cold plate to a pressure drop characterization test during the manufacturing process.

It should be noted that comparing Figure 6 and Figure 7 the server modules show different pressure drop even though they are connected in parallel. This behavior is due to the experimental procedures. In Figure 6, the flow meter introduces an extra pressure drop to the server module circuit. however, in Figure 7 the pressure drop is only measured for the server module without the effect of the flow meter. Ultimately, this does not change the conclusion that is the variation in the pressure drops of the server modules in Figure 7 causes the maldistribution in flow rate in Figure 6.

Figure 9 shows experimental measurements for the impact of different coolant temperatures on the pressure characteristics of the server module. The pressure drop increases 25% in average when the coolant temperature is decreased from 45°C to 20°C. Therefore, the required pumping power at a lower coolant temperature will be more than that at a higher temperature. Additionally, using coolant temperature of 45°C enhances the opportunity to use water side economizer and free cooling, which can lead to more savings.

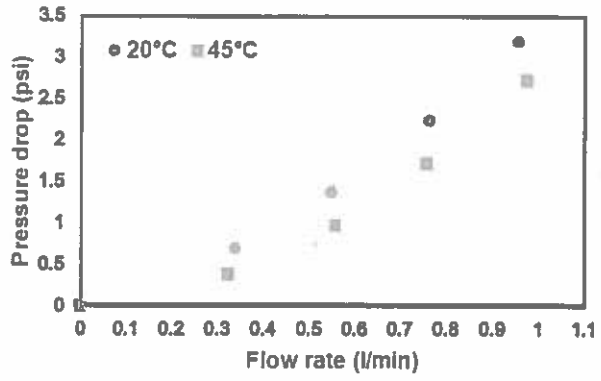

Figure 9: Impact of coolant temperature on the pressure drop

FLOW NETWORK ANALYSIS

In this part, the methodology to develop an accurate flow network model for the DLC rack is described. A flow network modeling (FNM) is used to predict the flow in pipe networks by representing the system as an electrical circuit. The flow in each branch in a system depends upon its resistance. The secondary loop of the DLC system is represented as a flow network using the commercial software Macroflow™ [24].

The pressure drop in the pipes is calculated using:

$$\Delta p = \left(\frac{f \times L}{D}\right)\left(\frac{\rho \times v^2}{2}\right) \qquad (1)$$

where f is the friction factor (function of Reynolds number and surface roughness), L is the pipe length (m), D is the hydraulic diameter (m), ρ is the fluid density (kg/m^3) and v is the fluid velocity (m/s). The software uses this equation to calculate the pressure drop in the connecting tubes between the CDM and the supply/return manifolds, and in the manifold module. Accurate measurements are taken for each of these parts and incorporated in the model.

The pressure drop in flow resistances is calculated using:

$$\Delta p = K\left(\frac{\rho \times v^2}{2}\right) \qquad (2)$$

The loss coefficient (K) for several components exists in the software library based on published literature [29, 30]. This feature of the library is used to calculate the pressure drop in the tubes bends, expansion/contraction from the manifold module to the server module and at the T-junctions of the manifold module. Also, the loss coefficient (K) of the actual CDM disconnects is obtained from the manufacturer and incorporated in the software.

The pressure drop in components with measured pressure drop as a function of flow rate is calculated using:

$$\Delta p = A \times Q + B \times Q^2 \qquad (3)$$

Where Q is the volumetric flow rate (m^3/s), and A and B are constants extracted from the curve fitting equation of the experimental data. We used this user defined function in the FNM software to model the pressure drop in the server modules. Polynomial curve fitting for the data in Figure 7 is incorporated in the software for server modules 1 to 14-2. The measured pressure drop includes the pressure drop in the corrugated hoses, dry-break quick disconnect plugs and socket, elbow fittings, and the micro-channel cold plate component.

Estimating the pump head and the internal pressure drop inside the CDM is required to complete the FNM for the DLC rack. Although the manufacturer head curves of the recirculation pumps (2 & 3) in Figure 10a are available, estimating the internal resistance requires destructive testing. Alternatively, the CDM head curve is introduced rather than the pump head curve. The CDM head curve represents the components 1-4 in Figure 10a using a single curve that can be incorporated in the FNM software. This curve can be measured experimentally by introducing the CDM to a variable external resistance (part (5) in Figure 10a), and measure the flow rate and pressure drop. The measured CDM head curve in Figure 10b presents the average results of three tests. This curve can be incorporated in the FNM software as a polynomial function. The previous steps show that the FNM mainly depends on the experimental measurements in this paper except for few flow resistances that are estimated from literature.

The flow network model is validated against experimental measurements. By changing the number of connected server modules to the DLC system, four scenarios can be considered: (a) server modules 1 to 14-2 (baseline) corresponding to 14.4 l/min pump flow (b) server modules 2 to13 corresponding to 12.3 l/min pump flow (c) server modules 1-2, 4, 6, 8, 10, 11, 13, 14-1and 14-2 corresponding to 11.5 l/min pump flow (d) server modules 1, 3, 5, 7, 9, 12, 14-1and14-2 corresponding to total pump flow of 10.4 l/min.

Figure 11 shows that the FNM shows good accuracy compared to measurements. The average error in predicting the flow rate in the server module is 2.5% while the maximum error

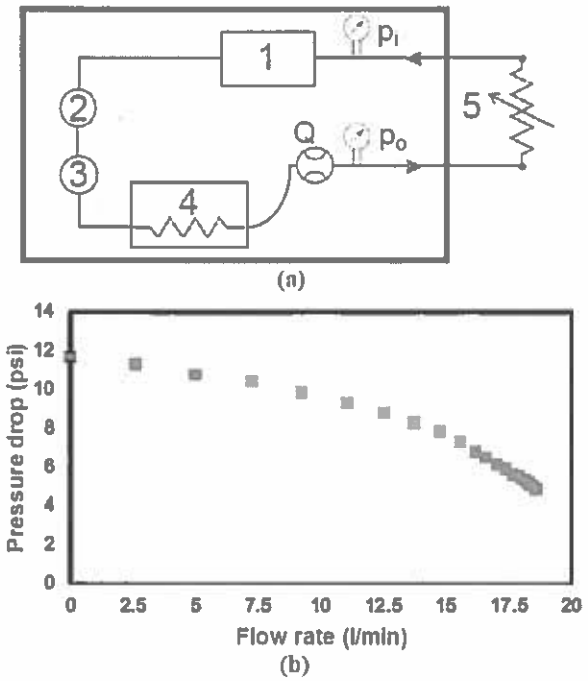

Figure 10: (a) Schematic of the CDU secondary loop (b) measured CDU head curve (1: coolant reservoir, 2&3: recirculation pumps, 4: liquid-liquid heat exchanger, 5: variable external resistance)

is 5.49%. The average error in predicting the pump flow rate (CDM flow) is 3.8% while the maximum error is 5.7%. The run time of the developed FNM is less than 10 seconds. The good accuracy of the model and its short run time make FNM a good tool for design, analysis, and optimization for DLC systems.

PRESSURE DROP ANALYSIS

In this section, the verified FNM and experimental measurements are used to understand the pressure drop distribution in the DLC rack. High pressure leads to more required pumping power, which prompts an increase in the cooling cost and reduces the data center energy efficiency. This analysis identify the high-pressure elements in the DLC system therefore future designs and optimization studies focus on these elements.

As indicated in the System Description section of this paper, there are three main modules in the DLC rack, which are the cooling distribution module (CDM), manifold module and the server module. In the first part of this section, we determine the relative pressure drop of each module with respect to the total pressure drop in the DLC system.

The used methodology to measure the CDM head curve to develop the FNM does not explicitly estimate the internal resistance of the CDM (heat exchanger, flow meter, reservoir, bends, fittings). The internal resistance of the CDM can be estimated using the measured CDM head curve and the pump's manufacturer head curve. Using the electronic-hydraulic analogy, an equivalent electrical circuit for the CDM is created, as shown in Figure 12a. In the electrical circuit, v_{cb} and v_{dc} represent the recirculation pumps head, v_{cd} and v_{ba} represent the pressure drop in the internal resistance, and v_{ae} represents the measured pressure drop in the external resistance. Applying Kirchhoff's voltage law (KVL), which is the directed sum of the electrical potential differences around any closed network is zero, in the denoted direction in Figure 12a yields:

$$v_{cb} + v_{dc} - v_{cd} - v_{ba} = 0 \qquad (4)$$

Internal pressure drop is calculated using:

$$(v_{cd} - v_{ba}) = v_{cb} + v_{dc} - v_{ae} \qquad (5)$$

The internal resistance of the CDM can be estimated at any pump flow rate, as shown in Figure 12b.

The pressure distribution in the DLC rack is shown in Figure 13. The rack in this case is equipped with 15 server modules (baseline scenario). The highest pressure drop in the rack is in the server module (56%). This finding is interesting, especially when it is compared to the second highest pressure drop in the CDM, which contains a heat exchanger, reservoir, flow meter and several fittings. The pressure drop in the supply/return manifolds is the lowest at 10% of the total pressure drop in the system.

Due to these findings, we conducted a deeper investigation of the server module. The pressure drop in the server module

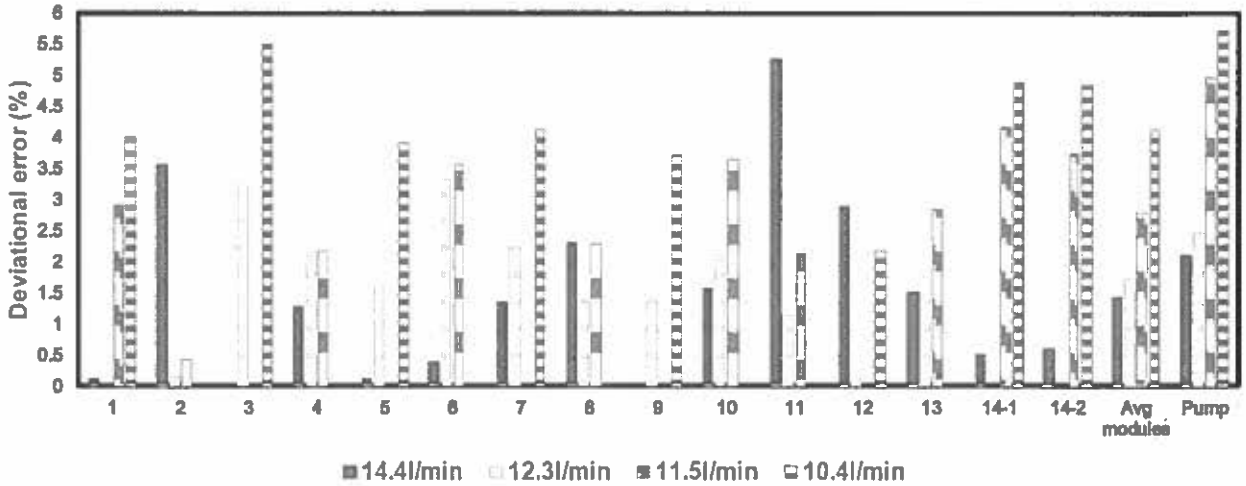

Figure 11: FNM verification against experimental data

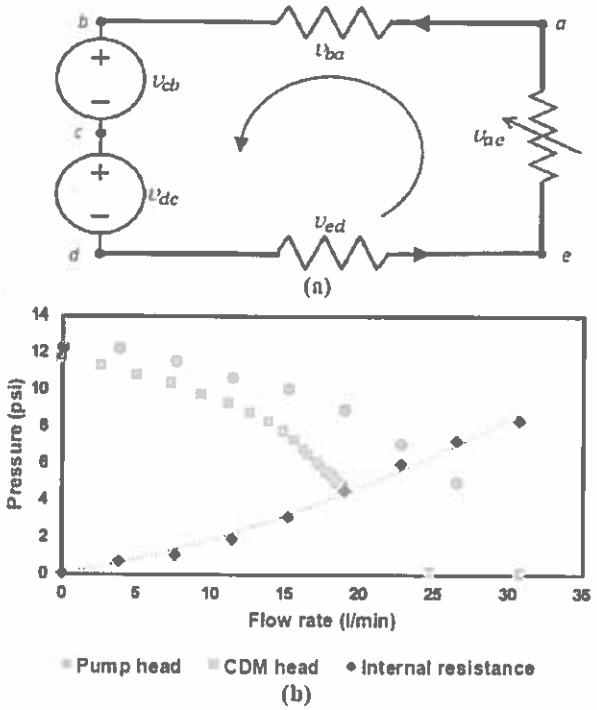

Figure 12: (a) Equivalent electrical circuit for the secondary loop of the CDM (b) Estimating the internal resistance of the CDM

The pressure drop in the server module consists of the pressure drop in the micro-channel cold plate and the pressure drop in the plumbing (corrugated hoses, disconnects, elbows). Destructive testing for the server module is performed by separating the micro-channel cold plate from the attached plumbing, as shown in Figure 14 (a,b). A brass pipe nipple is used to replace the cold plate in the server module to determine only the pressure drop in the plumbing, as shown in Figure 14b. The brass pipe nipple is carefully installed to avoid introducing extra pressure. This is done by using a smooth brass material and a nipple with the same diameter as the server module fittings.

The measured impedance curves for the server module and the plumbing part are shown in Figure 14c. The cold plate impedance is not measured as it requires installing extra couplings to be compatible with the sensors, which will produce unrealistic representation of the cold plate pressure drop. However, the cold plate pressure drop can be calculated by subtracting in the plumbing from the pressure drop in the server module, as shown in Figure 14c.

Figure 14 shows that the pressure drop in the server module plumbing is greater than that in the micro-channel cold plate. This finding is not intuitive as the cold plate contains channels with width as small as 100μm. The dry-break quick disconnects, corrugated hoses and elbows cause influential change in area and direction to the flow that exceeds the pressure drop in the micro-channels. Also, the flow in the plumbing part is found to be in the transitional regime for flow rate more than 0.8 l/min which increases the pressure drop.

The results in Figure 14 is used in the FNM of the rack. For

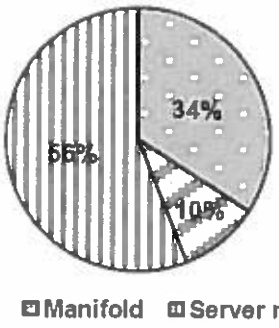

Figure 13: Pressure drop distribution in the rack

the same case in Figure 13, it is found that the pressure drop in the plumbing is 69% of the pressure drop in the server module and 31% only in the micro-channel cold plate. Since pressure drop in the server module is the highest in the rack (56%), the server module plumbing contributes by 39% of the pressure drop in the rack.

We showed in the pressure drop analysis the pressure drops in the modules of the DLC rack and their relative contribution to the total pressure drop. Pressure drop in plumbing of the server module is the highest among the other components. Their design to provide secured connections (by using dry-break quick disconnects) and flexibility due to room restriction inside

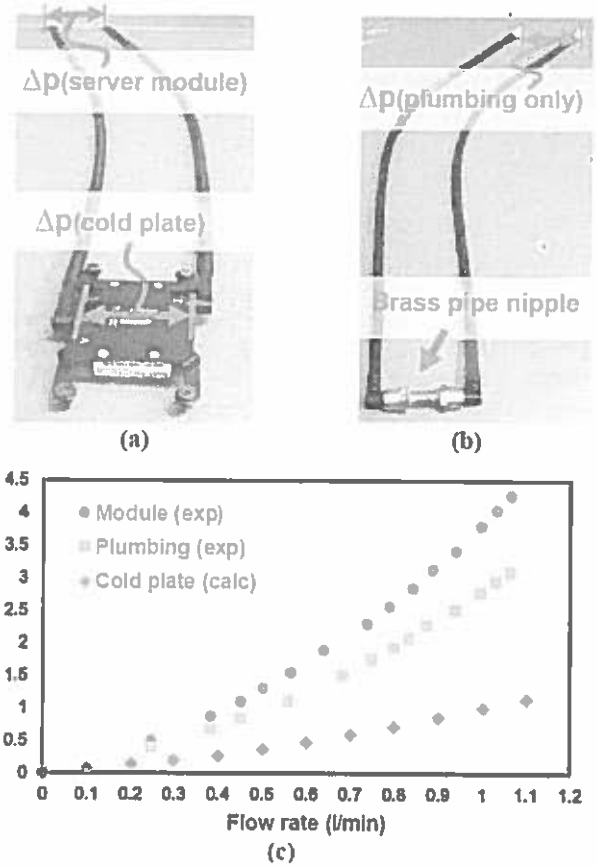

Figure 14: (a) Server module (b) Module plumbing (c) Measured and calculated flow resistances

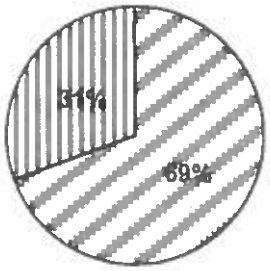

Figure 15: Pressure drop distribution in the server module

servers (by using corrugated hoses and elbows) came with a high pressure drop cost. These results are crucial for DLC designers to realize the substantial impact of using these elements. High pressure drop reduces the cooling system efficiency by increasing the required pumping power. Also, high pressure drops increase the stresses in these elements, which reduce their life span and make them vulnerable to failure.

The optimization of the DLC rack for energy efficiency should include the pressure drops. Optimized designs may take two paths: DLC system as a retrofit cooling solution or DLC in the design stage of the IT equipment. Optimization of DLC system as a retrofit solution may include fittings with gradual change in area and direction, and hoses with low friction and predetermined diameter to avoid turbulent flow. More dramatic designs include integrated liquid piping system in the IT equipment at the design stage. These designs eliminate the need for fittings and provide low resistance path inside a server. These integrated designs may not be tempting for commercial purposes.

SUMMARY AND CONCLUSIONS

This research provides a detailed experimental analysis for the pressure drop in a direct liquid cooled (DLC) rack. The main objective of this paper is to define the components with high pressure drops therefore they can be targeted in optimization studies. The pressure drop in the server module was found to cause the highest pressure drop among the coolant distribution module (CDM) and the manifold module. The liquid cooling server modules are designed to provide secured connections and flexibility, which lead to a high pressure drop cost.

This research also described a methodology to develop an accurate flow network model for the DLC rack and justify its accuracy. The average error in predicting the flow rate in 15 server modules and the CDM pump is 2.5% and 3.8%, respectively. The good accuracy of the model and its short run time make FNM a good tool for design, analysis, and optimization for DLC systems.

Flow maldistribution in the server modules was discovered experimentally and attributed to the manufacturing process of the micro-channel cold plate. The flow maldistribution is a potential risk on the reliability of the IT equipment by providing insufficient liquid flow.

REFERENCES

[1] U.S. Environmental Protection Agency (EPA). "Report to Congress on Server and Data Center Energy Efficiency Public Law 109-431." U.S. Environmental Protection Agency, ENERGY STAR Program, 2007.

[2] A. Shehabi, S. Smith, D. Sartor, R. Brown, M. Herrlin, J. Koomey, E. Masanet, N. Horner, I. Azevedo and W. Lintner. "United States Data Center Energy Usage Report." Ernest Orlando Lawrence Berkeley National Laboratory (LBNL), 2016.

[3] M. Iyengar, "Energy Consumption of Information Technology Data Centers," Journal of Electronics Cooling, vol. 16, no. 4, 2010.

[4] M. Stansberry and J. Kudritzki, "Uptime Institute 2012 Data Center Industry Survey," white paper, Uptime Institute, 2013.

[5] S. Alkharabsheh, J. Fernandes, B. Gebrehiwot, D. Agonafer, K. Ghose, A. Ortega, Y. Joshi and B. Sammakia, "A Brief Overview of Recent Developments in Thermal Management in Data Centers," Journal of Electronic Packaging, vol. 137, no. 4, p. 040801 (19 pages), 2015.

[6] S. Alkharabsheh, B. Sammakia and S. Shrivastava, "Experimentally Validated Computational Fluid Dynamics Model for a Data Center With Cold Aisle Containment," Journal of Electronic Packaging, vol. 137, no. 2, p. 021010 (9 pages), 2015.

[7] J. Siriwardana, S. Jayasekara and S. Halgamuge, "Potential of Air-side Economizers for Data Center Cooling: A case study for key Australian cities," Applied Energy, vol. 104, pp Pages 207-219, 2013.

[8] R. Schmidt, R. Chu, M. Ellsworth, M. Iyengar, D. Porter, V. Kamath and B. Lehman, "Maintaining Datacom Rack Inlet Air Temperatures with Water Cooled Heat Exchanger," in July 17-22, IPACK2005, San Francisco, CA, USA, 2005.

[9] S. Zimmermann, I. Meijer, M. Tiwari, S. Paredes, B. Michel and D. Poulikakos, "Aquasar: A Hot Water Cooled Data Center with Direct Energy Reuse," Energy, vol. 43, no. 1, pp. 237-245, 2012.

[10] D. L. Beaty, "Liquid Cooling--Friend or Foe," ASHRAE Transactions, vol. 110, no. 2, 2004.

[11] M. J. Ellsworth, L. A. Campbell, R. E. Simons, M. Iyengar and R. R. Schmidt, "The Evolution of Water Cooling for IBM Large Server Systems: Back to the Future.," in Thermal and Thermomechanical Phenomena in Electronic Systems (ITherm), 2008 IEEE Intersociety Conference on., Lake Buena Vista, Florida, 2008.

[12] "2014 Data Center Industry Survey," UptimeInstitute, 2014.

[13] M. Ellsworth and M. Iyengar, "Energy efficiency analyses and comparison of air and water cooled high performance servers," in ASME 2009 InterPACK Conference collocated with the ASME 2009 Summer Heat Transfer Conference and the ASME 2009 3rd

International Conference on Energy Sustainability, San Francisco, CA, USA, 2009.

[14] M. Iyengar, M. David, P. Parida, V. Kamath, B. Kochuparambil, D. Graybill, M. Schultz, M. Gaynes, R. Simons, R. Schmidt and T. Chainer, "Extreme energy efficiency using water cooled server inside a chiller-less data center," in IEEE Intersociety Conference on Thermal and Thermomechanical Phenomena in Electronic Systems, San Diego, CA, USA, 2012.

[15] M. David, M. Iyengar, P. Parida, R. Simons, M. Schultz, M. Gaynes, R. Schmidt and T. Chainer, "Impact of operating conditions on a chiller-less data center test facility with liquid cooled servers," in IEEE Intersocity Conference on Thermal and Thermomechanical Phenomena in Electronic Systems, San Diego, CA, USA, 2012.

[16] R. Miller, "Rise of Direct Liquid Cooling in Data Centers Likely Inevitable," Data Center Knowledge, 2014.

[17] "New Liquid Cooled HPC Cluster Launched," Electronics Cooling, 2016.

[18] L. Parnell, D. Demetriou and E. Zhang, "Combining Cooling Technology and Facility Design to Improve HPC Data Center Energy Efficiency," in Thermal and Thermomechanical Phenomena in Electronic Systems (ITherm), 2016 15th IEEE Intersociety Conference on, Las Vegas, NV, USA, 2016.

[19] H. Coles and S. Greenberg, "Direct Liquid Cooling for Electronic Equipment," Ernest Orlando Lawrence Berkeley National Laboratory, 2014.

[20] T. Cader, L. Westra, A. Marquez, H. McAllister and K. Regimbal, "Performance of a Rack of Liquid-Cooled Servers," ASHRAE Transactions, vol. 13, no. 1, pp. 101-114, 2007.

[21] K. Kelkar and S. Patankar, "Analysis and Design of Liquid-Cooling Systems Using Flow Network Modeling (FNM)," in ASME 2003 International Electronic Packaging Technical Conference and Exhibition (InterPACK), Maui, HI, USA , 2003.

[22] A. Radmehr and S. Patankar, "A Flow Network Analysis of a Liquid Cooling System that Incorporates Microchannel Heat Sinks," in Thermal and Thermomechanical Phenomena in Electronic Systems, Las Vegas, NV, USA, 2004.

[23] M. Ellsworth, "Flow Network Analysis of the IBM Power 775 Supercomputer Water Cooling System," in Thermal and Thermomechanical Phenomena in Electronic Systems (ITherm), 2014 IEEE Intersociety Conference on, Orlando, FL, USA, 2014.

[24] Innovative Research, Inc., "MacroFlow Users Manual," Innovative Research, Inc., 3025 Harbor Lane N., Plymouth, MN 55447, www.inres.com.

[25] "Direct Contact Liquid Cooling for the Datacenter- Can it be Simple, Low Cost, High Performance and Efficient?," Electronics Cooling Magazine, 2012.

[26] R. Millder and P. Mcginn, "CoolIT Systems Inc.," MIAX Options Exchange, Princeton, NJ, USA, 2014.

[27] B. Ramakrishnan, S. Alkharabsheh, Y. Hadad, B. Sammakia, P. Chiarot, M. Seymour and R. Tipton, "Experimental Characterization of a Cold Plate used in Warm Water Cooling of Data Centers," in 33th Semiconductor Thermal Measurement, Modeling & Management Symposium (SEMI-THERM), IEEE, San Jose, CA, USA, 2017.

[28] Y. Hadad, B. Ramakrishnan, S. Alkharabsheh, P. Chiarot and B. Sammakia, "Numerical Modeling and Optimization of a V-groove Warm Water Cold-Plate," in Semiconductor Thermal Measurement and Management Symposium (SEMI-THERM), IEEE, San Jose, CA, USA, 2017.

[29] I.E. Idelchik, Handbook of Hydraulic Resistance, FLorida: CRC Press, 1994.

[30] D. Miller, Internal Flow Systems, Texas: Gulf Publishing Company, 1990.